No. CHE77-00448 to F.A.C.) is gratefully acknowledged. The Varian XL-200 spectrometer was purchased with funds from the National Science Foundation (Grant No. CHE80-04246 to Purdue). This support is gratefully acknowledged.

Registry No. [$Re_2(\mu\text{-}H)_3H_2(PPh_3)_4(CN\text{-}t\text{-}Bu)_2]PF_6$, 86676-29-1; [$Re_2(\mu\text{-}H)_4H_4(PPh_3)_4]PF_6$, 86664-86-0.

Supplementary Material Available: Tables of all bond distances and angles, anisotropic thermal parameters, least-squares planes for all phenyl rings, and observed and calculated structure factors (52 pages). Ordering information is given on any current masthead page.

Contribution from the Institute of Inorganic Chemistry, University of Münster, D-4400 Münster, Federal Republic of Germany, and Chemistry Department A, Technical University of Denmark, DK-2800 Lyngby, Denmark

$NbAlCl_8$: A Molecular Dinuclear Complex in the Solid, Melt, and Vapor Phases. Synthesis, Crystal Structure, and Raman Spectra

BERNT KREBS,*[1a,e] HOLGER JANSSEN,[1a] NIELS J. BJERRUM,*[1b] ROLF W. BERG,[1b]
and G. N. PAPATHEODOROU[1c,d]

Received March 10, 1983

Crystalline $NbAlCl_8$ was prepared as a new type of dinuclear halide complex by the direct reaction of Al_2Cl_6 with Nb_2Cl_{10} at ~200 °C in evacuated sealed glass ampoules. The yellow compound is orthorhombic, space group *Cmcm*, with a = 8.016 (2) Å, b = 17.139 (4) Å, c = 8.116 (2) Å, V = 1115.1 Å^3, D_{measd} = 2.40 (2) g·cm^{-3}, and D_{calcd} = 2.403 g·cm^{-3} for Z = 4. The crystal and molecular structure determination was based on three-dimensional X-ray diffractometer data refined to a final conventional R factor of 0.030 for 639 independent reflections with $I \geq 2\sigma(I)$. The crystals contain dinuclear $Cl_4NbCl_2AlCl_2$ molecules with *mm* symmetry, consisting of an $AlCl_4$ tetrahedron sharing a common edge with a distorted $NbCl_6$ octahedron. Al–Cl bond lengths of 2.078 (2) and 2.200 (2) Å and Nb–Cl bond lengths of 2.219 (1), 2.288 (1), and 2.643 (1) Å were observed. The Nb–Cl bridge bonds are longer than in the Nb_2Cl_{10} molecule, thus indicating a higher Lewis acidity of $AlCl_3$ compared to that of $NbCl_5$. Polarized Raman spectra of $NbAlCl_8$ single crystals were obtained at room temperature. The factor-group analysis of vibrations in crystalline $NbAlCl_8$ was used for the assignment of the observed Raman bands. Raman spectra of melt mixtures of $NbCl_5$ with $AlCl_3$ at 235 °C were characterized by a superposition of bands due to Al_2Cl_6(l), Nb_2Cl_{10}(l), and $NbCl_5$(l), together with $NbAlCl_8$(l). Measurements of relative Raman band intensities in the mixtures showed two strongly polarized bands at 416 and 364 cm^{-1} and other weaker bands due to $NbAlCl_8$ complexes present in the melts. Raman spectra of vapors over the liquid mixtures at temperatures between 235 and 350 °C were mainly due to Al_2Cl_6(g) and $NbCl_5$(g) molecules. Two new polarized bands observed in the spectra at 418 and 369 cm^{-1} were attributed to the formation of the $NbAlCl_8$ gaseous molecule.

Introduction

The chlorides and bromides of aluminum, gallium, and indium are able to form ternary complex halides with a large number of other metal and nonmetal halides in the gas phase or in the condensed state.[2] These complex halides sometimes occur as molecules; as volatile "gas complexes" they are important for many types of chemical transport reactions,[2,3] e.g. in the case of a halide transport according to

$$MCl_x(\text{solid}) + 0.5nAl_2Cl_6(\text{gas}) \rightleftarrows MCl_x{\cdot}nAlCl_3(\text{gas})$$

On the other hand, they can form various aggregates in the solid state, in which more or less pronounced heteropolar bonding is present according to the Lewis acid and base properties of the components. For Al_2Cl_6 (or just $AlCl_3$), by far the most important of the mentioned complex-forming trihalides, a considerable number of ternary compounds with dihalides and tetrahalides have been isolated as solids, and some of them are structurally well characterized by X-ray diffraction. The latter include trinuclear $CuAl_2Cl_8$[4] and $PdAl_2Cl_8$[5] as well as the two- or three-dimensionally polymeric compounds $CoAl_2Cl_8$,[6] $NiAl_2Cl_8$,[7] $SCl_3^+AlCl_4^-$,[8] $SeCl_3^+AlCl_4^-$,[9] and $TeCl_3^+AlCl_4^-$.[10] Little is known about complex formation in the solid among two trichlorides.

Concerning possible complex formation between trihalides and pentahalides, however, all chemical and structural knowledge is restricted to results of vibrational, electron, and mass spectroscopic as well as thermoanalytic and potentiometric work. The gas complexes $UAlCl_8$[11] and $TaAlCl_8$[12] have been shown to exist, ionic structures $PCl_4^+MCl_4^-$ are derived from vibrational spectra of the PCl_5–MCl_3 systems (M = B, Al, Ga),[13] and the complex $NbGaCl_8$ was postulated from liquid and solid-state Raman spectra[14] and by DTA measurements.[15] Some evidence on the nature of possible complexes between $NbCl_5$ and $AlCl_3$ is obtained from investigations in KCl–$AlCl_3$–$NbCl_5$ melts[16] and from mass spectroscopy in the gas phase.[12] In the following we report the preparation and characterization of the crystalline 1:1 complex between $NbCl_5$ and $AlCl_3$, which is the first example of structural analysis of this novel type of binuclear molecular addition compound. Also, Raman spectra of the complex in the solid, liquid, and gaseous phases are obtained.

Synthesis of Crystalline $NbAlCl_8$

Because of the extreme sensitivity of the compounds toward hydrolysis and partial oxidation, all operations had to be done under exclusion of moisture and oxygen by means of standard glovebox and sealed-cell techniques. The starting materials used for the synthesis

---

(1) (a) University of Münster. (b) Technical University of Denmark. (c) University of Patras, Patras, Greece. (d) Visiting Professor at TUD in 1982. (e) Visiting Professor at TUD in 1981.

(2) Papatheodorou, G. N. *Curr. Top. Mater. Sci.* **1982**, *10*, 249.

(3) Schäfer, H. *Angew. Chem.* **1976**, *88*, 775; *Angew. Chem., Int. Ed. Engl.* **1976**, *15*, 713.

(4) Schäfer, H.; Binnewies, M.; Laumanns, R.; Wächter, H. *Z. Anorg. Allg. Chem.* **1980**, *461*, 31.

(5) Lenhard, W.; Schäfer, H.; Hürter, H.-U.; Krebs, B. *Z. Anorg. Allg. Chem.* **1981**, *482*, 19.

(6) Ibers, J. A. *Acta Crystallogr.*, **1962**, *15*, 967.

(7) Brynestad, J.; Yakel, H. L.; Smith, G. P. *Inorg. Chem.* **1970**, *9*, 686.

(8) Krebs, B.; Hein, M.; Janssen, H. *Z. Naturforsch., B: Anorg. Chem., Org. Chem.*, in press. Hein, M. Doctoral Thesis, Münster, 1979.

(9) Stork-Blaisse, B. A.; Romers, C. *Acta Crystallogr., Sect. B: Struct. Crystallogr. Cryst. Chem.* **1971**, *B27*, 386.

(10) Krebs, B.; Buss, B.; Altena, D. *Z. Anorg. Allg. Chem.* **1971**, *386*, 257. Krebs, B.; Buss, B.; Berger, W. *Ibid.* **1973**, *397*, 1.

(11) Gruen, D. M.; McBeth, R. L. *Inorg. Chem.* **1969**, *8*, 2625.

(12) Schäfer, H.; Flörke, U. *Z. Anorg. Allg. Chem.* **1981**, *479*, 89.

(13) Gerding, H.; Duinker, J. C. *Rev. Chim. Miner.* **1966**, *3*, 815. Carlson, G. L. *Spectrochim. Acta* **1963**, *19*, 1291.

(14) Okon, G. *Z. Anorg. Allg. Chem.* **1980**, *469*, 68.

(15) Fedorov, P. I.; Khagleeva, L. P. *Russ. J. Inorg. Chem.* (*Engl. Transl.*) **1967**, *12*, 430. Chikanov, N. D. *Ibid.* **1968**, *13*, 1349.

(16) von Barner, J. H.; Bjerrum, N. J.; Smith, G. P. *Acta Chem. Scand., Ser. A* **1978**, *A32*, 837.

Table I. Coordinates of the Atoms and Anisotropic Temperature Factor Coefficients with Standard Deviations[a] for $NbAlCl_8$

	pos	sym	x	y	z	B_{11}	B_{22}	B_{33}	B_{12}	B_{13}	B_{23}
Nb	4c	*mm*	0.0	0.11026 (3)	0.25	2.53 (3)	1.64 (2)	2.54 (3)	0.0	0.0	0.0
Al	4c	*mm*	0.0	0.31627 (12)	0.25	2.70 (9)	1.90 (8)	3.32 (9)	0.0	0.0	0.0
Cl(1)	8g	*m*	0.20516 (16)	0.23099 (7)	0.25	2.23 (5)	2.27 (4)	4.93 (7)	0.01 (4)	0.0	0.0
Cl(2)	8g	*m*	0.21489 (19)	0.02863 (8)	0.25	3.38 (6)	2.76 (5)	5.65 (8)	0.85 (5)	0.0	0.0
Cl(3)	8f	*m*	0.0	0.13221 (8)	0.52805 (18)	4.75 (8)	4.16 (6)	2.73 (6)	0.0	0.0	0.07 (5)
Cl(4)	8f	*m*	0.0	0.38144 (9)	0.03408 (23)	4.47 (8)	4.27 (7)	4.88 (8)	0.0	0.0	1.85 (6)

[a] The anisotropic temperature factors are defined as $\exp[-0.25(B_{11}a^{*2}h^2 + B_{22}b^{*2}k^2 + B_{33}c^{*2}l^2 + 2B_{12}a^*b^*hk + 2B_{13}a^*c^*hl + 2B_{23}b^*c^*kl)]$.

of the complex compound were prepared and purified as follows.

$AlCl_3$. Aluminum chloride was prepared from Al strips (Merck, p.A.) by chlorination in a flow system, the colorless product being sublimed under a N_2 stream.

AlSCl. Following earlier preparations,[17,18] we obtained aluminum sulfide chloride by reacting equimolar amounts of aluminum strips and sulfur (p.A.) with an excess of $AlCl_3$ (maximum 10 bar) during several days in an evacuated sealed borosilicate glass tube at 300 °C. Excess $AlCl_3$ and sulfur were removed by sublimation from the pure colorless AlSCl, which forms very fine colorless hairlike crystals.

$NbCl_5$. Niobium powder (Starck, p.A.) was reacted with a stream of dry chlorine under moderate heating; the resulting niobium pentachloride was purified by distillation under a Cl_2 atmosphere. Two methods were employed for the synthesis of the yellow crystalline 1:1 complex between $AlCl_3$ and $NbCl_5$. The first one (method a), consisting of the reaction of AlSCl with $NbCl_5$, originated from experiments to obtain single crystals of AlSCl by chemical transport according to the possible reaction

$$AlSCl(solid) + NbCl_5(gas) \rightleftarrows {}^1/_2Al_2Cl_6(gas) + NbSCl_3(gas)$$

which, however, led to the formation of $NbAlCl_8$ under the conditions chosen for the reaction (temperature as low as 190–200 °C). The second, more direct method of preparation, method b, used stoichiometric quantities of the binary halides as starting materials according to

$$NbCl_5 + AlCl_3 \rightarrow NbAlCl_8$$

and produced the crystalline binuclear complex with slow cooling. This preparation of $NbAlCl_8$ is in contrast to the simple eutectic phase diagram of the $AlCl_3$–$NbCl_5$ system available in the literature[19] and suggests a peritectic intermediate $NbAlCl_8$ phase that escaped attention because of low thermal effect. In a similar way, by reaction of the corresponding binary halides the crystalline molecular complexes $NbAlBr_8$, $TaAlCl_8$, and $TaAlBr_8$ seem to be formed.[20] Both methods are suitable for the production of good single crystals. The melting point of pure $NbAlCl_8$ is 139.7 °C.

Determination of Crystal Structure

Single-Crystal X-ray Investigations. Collection and Reduction of Intensity Data. From Weissenberg and precession photographs the crystals were shown to be *C*-centered orthorhombic, the reflections *hkl* with $h + k \neq 2n$ and $h0l$ with $l \neq 2n$ being systematically absent. The extinctions are consistent with the space group $Cmc2_1$ (No. 36), $C2cm$ (No. 40, standard setting $Ama2$), and $Cmcm$ (No. 63). The centrosymmetric $Cmcm$ was chosen as the correct one on the basis of the statistical distribution of the F values and was confirmed by the successful refinement of the structure. Precise unit-cell dimensions with standard deviations were derived from a least-squares fit to the four-circle diffractometer coordinates of 16 reflections. The refined unit cell constants are $a = 8.016$ (2) Å, $b = 17.139$ (4) Å, $c = 8.116$ (2) Å, and $V = 1115.1$ Å^3, with $D_{measd} = 2.40$ (2) g·cm^{-3} (flotation) and $D_{calcd} = 2.403$ g·cm^{-3} for $Z = 4$ $NbAlCl_8$. A crystal needle of the size 0.08 × 0.08 × 0.40 mm was used for the intensity measurements, the needle axis (identical with the crystallographic c axis) being approximately aligned along the ϕ axis of the diffractometer.

Table II. Observed and Calculated X-ray Powder Diagram for $NbAlCl_8$

hkl	d_{obsd}, Å	d_{calcd}, Å	rel I_{obsd}
110	7.338	7.334	55
021	5.854	5.852	45
111	5.417	5.412	100
040	4.287	4.285	15
200	4.062	4.058	22
131	4.033	4.036	28
002	4.003	4.008	20
041	3.782	3.779	10
112	3.517	3.517	20
150	3.158	3.158	12
240	2.947	2.946	48
023	2.551	2.551	12
113	2.512	2.511	12
152	2.478	2.480	16
242	2.375	2.374	8
331	2.339	2.339	8
261	2.244	2.243	15
223	2.159	2.160	6
350	2.123	2.124	6
400	2.028	2.029	8
004	2.004	2.004	8
352	1.876	1.876	12
263	1.757	1.759	8
192	1.684	1.683	5
244	1.656	1.657	8

(Most of the crystals grown were flat needles with the needle axis along c and with b perpendicular to the largest face.) The intensities of a complete set of 1424 reflections (two octants) up to $(\sin\theta)/\lambda = 0.64$ Å^{-1} were measured at 20 °C with a Syntex $P2_1$ four-circle diffractometer (Mo Kα radiation, $\lambda = 0.71069$ Å, parallel graphite monochromator, 2θ–θ scan mode, intensity-dependent variable scan rate of 3.0–29.3° min^{-1}, scan range in 2θ of 2.0–2.5°, and reference reflection every 50 reflections). The intensities were corrected empirically for absorption by registration of scans around the diffraction vectors of five selected reflections, transmission factors being larger than 0.86 ($\mu = 29.6$ cm^{-1} for Mo Kα). After averaging over symmetry-related data, the remaining 703 symmetry-independent intensities were corrected for Lorentz and polarization effects (Lp). A Wilson plot was calculated. A total of 64 of the reflections that had $I \leq 1.96\sigma(I)$ were considered as being unobserved and were excluded from the calculation ($w = 0$). The variance of I was calculated as $\sigma^2(I) = S + (B_1 + B_2)(t_S/2t_B)^2$, where S, B_1, and B_2 are the scan and individual background counts and where t_S and t_B are the counting times ($t_B = t_S/2$ was used).

Solution and Refinement of the Structure. The structure was solved from the Patterson synthesis. Besides the Nb atom, five of the eight Cl atoms could be derived directly; the rest of the atoms were obtained from a subsequent difference Fourier map. The same structural solution was reached by direct multisolution methods, with the EXTL version of the MULTAN program system. Several cycles of isotropic and anisotropic full-matrix least-squares refinement led to convergence (maximum shift/error: 0.01) and yielded final unweighted and weighted R values of $R_1 = \sum(||F_o| - |F_c||)/\sum|F_o| = 0.030$ and $R_2 = [\sum w(|F_o| - |F_c|)^2/\sum w|F_o|^2]^{1/2} = 0.033$. The quantity minimized was $\sum w(|F_o| - |F_c|)^2$ with $1/w = \sigma^2(F_o) + (0.008|F_o|)^2$ and $\sigma(F_o) = \sigma(I)/(2|F_o|Lp)$. The final goodness of fit $[\sum w(|F_o| - |F_c|)^2/(n_o - n_v)]^{1/2}$ with $n_o = 639$ observations and $n_v = 33$ variables was 1.81. The final difference Fourier map was featureless.

Scattering factors for neutral Nb, Al, and Cl, being corrected for anomalous dispersion, were taken as compiled in ref 21.

---

(17) Hagenmuller, P.; Rouxel, J.; David, J.; Colin, A.; LeNeindre, B. *Z. Anorg. Allg. Chem.* **1963**, *323*, 1.

(18) Berg, R. W.; von Winbush, S.; Bjerrum, N. J. *Inorg. Chem.* **1980**, *19*, 2688.

(19) Niselson, L. A.; Pustilnik, A. I.; Gavrilov, O. R.; Rodin, V. A. *Russ. J. Inorg. Chem.* (*Engl. Transl.*) **1965**, *10*, 1271.

(20) Detailed investigations are in progress.

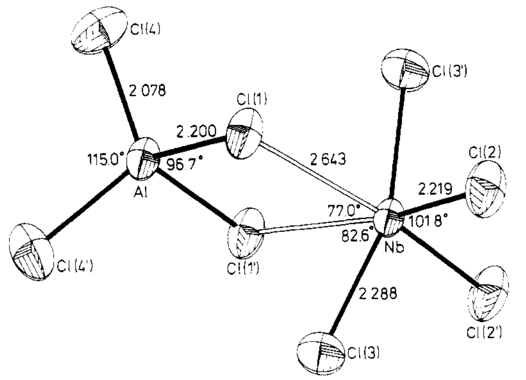

Figure 1. The $NbAlCl_8$ molecule in the crystal with bond lengths (Å) and angles (deg). Vibrational ellipsoids are scaled to 50% probability.

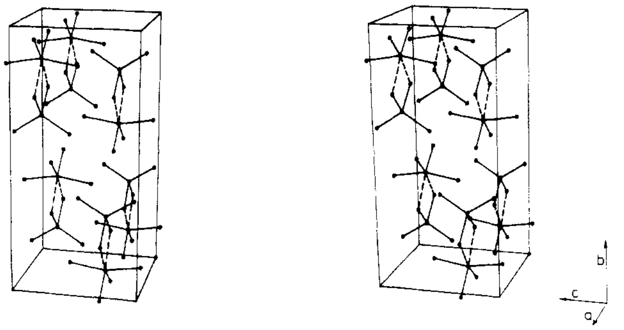

Figure 2. Stereoscopic drawing of the unit cell of $NbAlCl_8$.

The final atomic coordinates and anisotropic thermal parameters are given in Table I. The table of observed and calculated structure factors is available as supplementary material.[22]

X-ray Powder Diagram. The Guinier–Simon technique with monochromated Cu Kα radiation was used for the registration of the powder diagram (Table II, standard Si). As a check, the pattern was calculated from the single-crystal structure data. The d_{obsd} values and the relative intensities of the powder diagram are given in Table II together with the corresponding d_{calcd} values from the single-crystal data.

Crystal Structure

The structure consists of an arrangement of isolated dinuclear $Cl_4NbCl_2AlCl_2$ molecules with *mm* (C_{2v}) symmetry; there are no significant intermolecular bonding interactions. An ellipsoid plot of the molecule is shown in Figure 1; a list of interatomic distances and bond angles with standard deviations is given in Table III. The bond lengths were corrected for rigid-body librational motion of the molecule. Figure 2 gives a three-dimensional indication of the special kind of packing in a stereo plot of the unit cell (see also Figure 3 and the discussion below).

Table III. Interatomic Distances (Å) and Bond Angles (deg) with Standard Deviations for $NbAlCl_8$

	intramolecular dist	corrected
Nb–Cl(1)	2.643 (1) (2×)	2.651
Nb–Cl(2)	2.219 (1) (2×)	2.228
Nb–Cl(3)	2.288 (1) (2×)	2.301
Al–Cl(1)	2.200 (2) (2×)	2.209
Al–Cl(4)	2.078 (2) (2×)	2.091
Nb···Al	3.531 (2)	
Cl(3)···Cl(4)[a]	4.301 (2)	

	angle	Cl···Cl dist
Cl(1)–Nb–Cl(1)[a]	76.96 (5)	3.289 (2)
Cl(1)–Nb–Cl(2)	90.61 (4)	3.469 (2) (2×)
Cl(1)–Nb–Cl(2)[a]	167.56 (4)	4.834 (2) (2×)
Cl(1)–Nb–Cl(3)	82.60 (4)	3.265 (2) (4×)
Cl(2)–Nb–Cl(2)[a]	101.83 (5)	3.445 (2)
Cl(2)–Nb–Cl(3)	95.95 (4)	3.348 (2) (4×)
Cl(3)–Nb–Cl(3)[b]	161.07 (6)	4.513 (2)
Cl(1)–Al–Cl(1)[a]	96.74 (8)	3.289 (2)
Cl(1)–Al–Cl(4)	110.92 (7)	3.525 (2) (4×)
Cl(4)–Al–Cl(4)[b]	114.98 (9)	3.505 (3)
Nb–Cl(1)–Al	93.15 (5)	

[a] Symmetry transformation: $-x, y, z$. [b] Symmetry transformation: $-x, y, {}^1/_2 - z$.

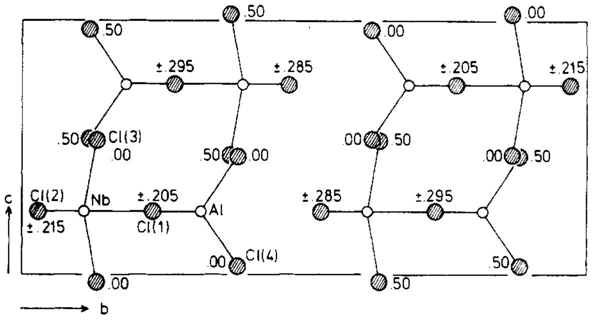

Figure 3. Packing of the chlorine atoms in the crystal structure of $NbAlCl_8$ (projection of the unit cell along *a* with *x* coordinates indicated).

Within the $NbAlCl_8$ molecular unit, the $AlCl_4$ tetrahedron shares a common edge with the $NbCl_6$ octahedron. Although $UAlCl_8$ has been found previously,[11] this appears to be the first example where the crystal structure of this novel dinuclear molecular unit type has been convincingly characterized. It is of special interest to compare the structural properties of the ternary compound with those of the corresponding binary dinuclear parent molecules Nb_2Cl_{10} and Al_2Cl_6. In the strongly distorted $NbCl_6$ octahedron of $NbAlCl_8$ the bridging Nb–Cl bonds are significantly longer than in Nb_2Cl_{10}[23] (2.643 (1) vs. 2.555 (6) Å) with a corresponding shortening of the equatorial Nb–Cl bonds in the plane of the central $AlCl_2Nb$ ring (2.219 (1) vs. 2.250 (6) Å) as well as of the axial Nb–Cl bonds perpendicular to the ring (2.288 (1) Å in $NbAlCl_8$ vs. 2.302 (5) Å in Nb_2Cl_{10}). As is to be expected, in both compounds the bonds trans to the bridge bonds are slightly shorter than the axial ones. In both cases the axial Nb–Cl bonds are bent toward the center of the molecule, evidently by ligand–ligand repulsion with the equatorial chlorine atoms (see also ref 24). The lengthening of the Nb–Cl bridge bonds in $NbAlCl_8$ compared to those in Nb_2Cl_{10} can be seen as a measure of the relative Lewis acidities of $AlCl_3$ and $NbCl_5$, the stronger interaction of Al with the bridging Cl atom indicating the slightly higher acidity at this side. The Cl–M–Cl angular distortions necessary to form the bridge bonds are ~13° from the ideal tetrahedral and octahedral values at both Al and Nb, respectively (Table III). The Al–Cl bond length distribution in the $AlCl_4$ tetrahedron, with significantly longer bridge bonds than terminal ones (2.200 (2) vs. 2.078 (2) Å), however, shows that the bonding character of the compound is still far from the limiting case $NbCl_4^+AlCl_4^-$ and that a "covalent" description like $Cl_4NbCl_2AlCl_2$ is more appropriate. Very similar distortions of the $AlCl_4$ tetrahedra are observed in gaseous Al_2Cl_6, where the bridge and terminal bond lengths were determined to be 2.21 (4) and 2.06 (4) Å,[25] and in the crystalline complexes $CoAl_2Cl_8$ (polymeric, 2.17 (1), 2.11 (2) Å),[6]

---

[21] "International Tables for X-ray Crystallography"; Kynoch Press: Birmingham, England, 1974; Vol. IV, p 99 ff.

[22] The computations were done on a Data General Eclipse S/200 computer using programs (partially modified) of the Syntex EXTL system and the SHELXTL program system of G. M. Sheldrick.

[23] Zalkin, A.; Sands, D. E. *Acta Crystallogr.* **1958**, *11*, 615.

[24] Krebs, B.; Sinram, D. *Z. Naturforsch., B: Anorg. Chem., Org. Chem.* **1980**, *35B*, 12.

[25] Palmer, K. J.; Elliott, N. *J. Am. Chem. Soc.* **1938**, *60*, 1852.

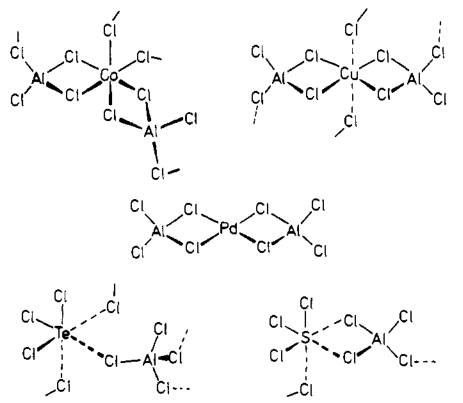

Figure 4. Schematic structures of the 1:2 adducts of $AlCl_3$ with $CoCl_2$,[6] $CuCl_2$,[4] and $PdCl_2$[5] and the 1:1 adducts with $TeCl_4$[10] and SCl_4.[8] $SeCl_3{}^+AlCl_4{}^-$[9] is similar to $TeCl_3{}^+AlCl_4{}^-$.

$CuAl_2Cl_8$ (trinuclear units, weak intermolecular Cu–Cl bonds, 2.20 (1), 2.09 (1) Å),[4] and $PdAl_2Cl_8$ (trinuclear molecules, 2.212 (2), 2.075 (2) Å).[5] A closer approximation to an ionic structure is observed in the 1:1 adducts between the chalcogen(IV) halides and $AlCl_3$, where the "bridge" and "terminal" Al–Cl bonds are closer to the value of 2.12–2.13 Å of the regular tetrahedral $AlCl_4{}^-$ ion:[26] 2.139 (2) and 2.122 (2) Å for $SCl_3{}^+AlCl_4{}^-$,[8] 2.14 (1) and 2.11 (1) Å for $SeCl_3{}^+AlCl_4{}^-$,[9] and 2.142 (2) and 2.087 (2) Å for $TeCl_3{}^+AlCl_4{}^-$.[10] Figure 4 shows the structures of these complexes.

It is interesting to note that, caused by the distortive intramolecular forces within the $NbAlCl_8$ molecules, the packing of the chlorine atoms in the crystal structure is closer to a distorted body-centered cubic than to a close-packed arrangement. Figure 3 shows a projection of the packing with the distorted bccub pseudocell having its axes parallel to *a*, *b*, and *c* of the $NbAlCl_8$ unit cell and with the ABABAB layers of a distorted hcp arrangement running parallel to (021) of the $NbAlCl_8$ cell. The intra- and intermolecular Cl···Cl distances (Table III and supplementary material) indicate the bccub description to be the more appropriate one.

Raman Spectra and Vibrational Analysis of Crystalline $NbAlCl_8$

Raman spectra were measured at room temperature on polycrystalline samples prepared by the two preparative methods (a and b) and on crystals formed by sublimation inside closed cells. The cells were made from quartz or borosilicate tubing (8–20 mm i.d.).[27] For recording of the spectra, krypton and argon ion lasers (15 and 4 W) were used. The scattered light was collected at an angle of 90°, analyzed with a Polaroid-sheet polarizer, giving polarized (||, vertical–vertical polarization) and depolarized (|⊥; vertical–horizontal polarization) spectra for the applied horizontal scattering plane), and sent through a 90° image rotator (vertical entrance slit) and through a polarization scrambler. The spectrometer was a JEOL JRS-400D 0.4-m double monochromator equipped with a −10 °C cooled extended S-20 photomultiplier and a photon-counting system. The spectrometer was calibrated within ±1 cm^{-1} with a Ne-discharge lamp, and bands were recorded also in the anti-Stokes spectrum. The recorded spectra (number of bands, their frequencies and relative intensities) were essentially identical, irrespective of the method of preparation and irrespective of the excitation wavelength (647.1, 514.5, or 488.0 nm). Our best obtained polarized crystal spectra are shown in Figure 5. Similar spectra of slightly inferior quality were obtained with use of the 647.1-nm krypton line (1 W). The crystal used for obtaining Figure 5 was grown by sublimation at ca. 200 °C inside a closed ampule and had the shape of a thin square plate. The excitation beam entered the crystal approximately perpendicular to the large face, which according to the usual habit of the $NbAlCl_8$ crystal should be (010); i.e. the beam came along the crystallographic *b* axis. The scattered light could only be satisfactorily collected in one perpendicular direction, because of the shape of the ampule. By comparison with less well-resolved spectra of two other oriented, flat-needle crystals (probably elongated along the crystallographic *c* axis [001], according to the usual habit),

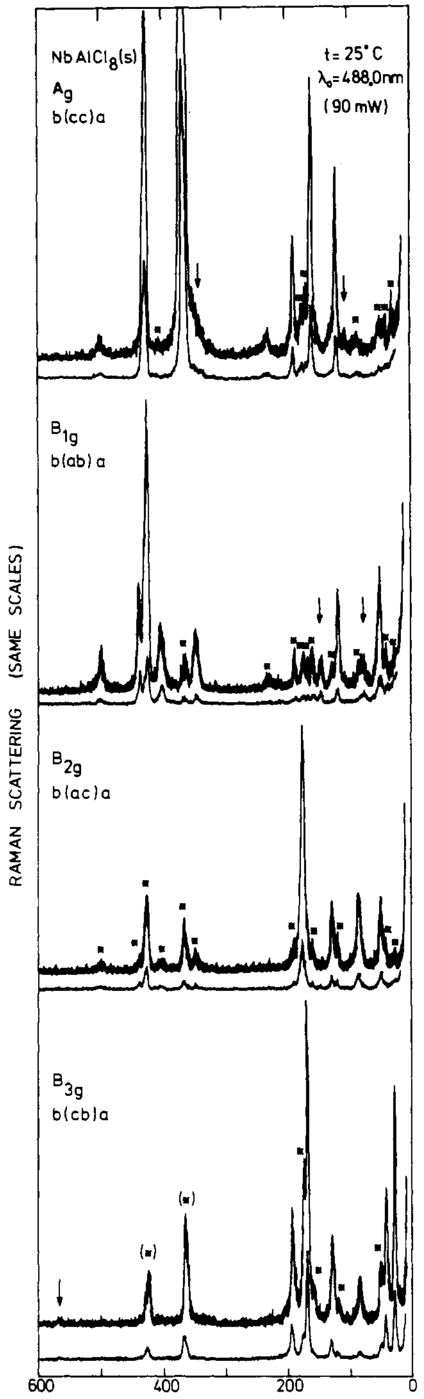

Figure 5. Two sets of oriented crystal spectra of $NbAlCl_8$ at room temperature, each set with the same scale (resolution ~2 cm^{-1}, scanning speed 25 cm^{-1} min^{-1}): *, band leaking from another orientation; (*), perhaps a band leaking from another orientation; ↓, band of the particular symmetry.

---

(26) Mairesse, G.; Barbier, P.; Wignacourt, J.-P. *Acta Crystallogr., Sect. B: Struct. Crystallogr. Cryst. Chem.* **1979**, *B35*, 1573.

(27) For further experimental details, see: (a) Papatheodorou, G. N.; Capote, M. A. *J. Chem. Phys.* **1978**, *69*, 2067. (b) Papatheodorou, G. N. *NBS Spec. Publ.* (*U.S.*) **1979**, *No. 561*.

Table IV. Symmetry Distribution of Internal Group Vibrations in a $NbAlCl_8$ Molecule of C_{2v} Symmetry[a]

	A_1	A_2	B_1	B_2
$NbCl_4$ terminal str	2		1	1
$AlCl_2$ terminal str	1		1	
Cl bridge str-bend	2			2
$AlCl_2$ scissors	1			
$NbCl_4$ scissors	2	1	1	1
$AlCl_2$ twist		1		
$AlCl_2$ rock, wag			1	1
$NbCl_4$ twist		1		
$NbCl_4$ rock, wag			1	1
Nb···Al str	1			
$NbCl_2Al$ plane bend			1	

[a] The molecule is oriented in the *xyz* coordinate system such that the C_2 symmetry axis is taken along *z* and the $NbCl_2Al$ skeleton is in the *yz* plane.

Table V. Correlation Diagram[a] for $NbAlCl_8$ Vibrations

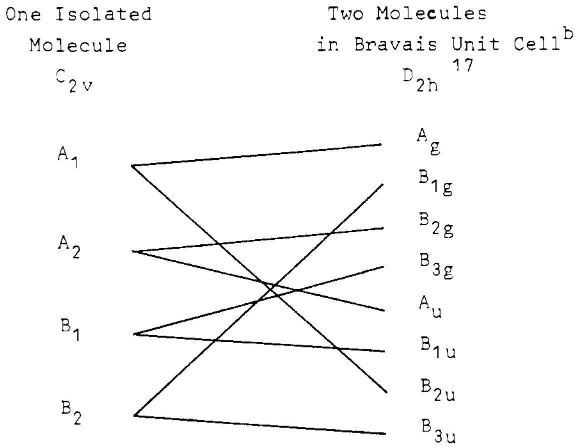

[a] The site symmetry is the same as the point symmetry of the free molecule. [b] The axes of the unit cell are taken so that C_2 rotation is along *y* and the $NbCl_2Al$ skeleton is in the *xy* plane.

Table VI. Unit Cell Group Analysis of Vibrations in Crystalline $NbAlCl_8$[a]

D_{2h}^{17}	A_g	B_{1g}	B_{2g}	B_{3g}	A_u	B_{1u}	B_{2u}	B_{3u}
N_i	9	6	3	6	3	6	9	6
T_a	0	0	0	0	0	1	1	1
T	1	1	0	1	0	0	0	0
R	0	1	1	1	1	1	0	1
Raman activity	*xx, yy, zz*	*xy*	*xz*	*yz*				
IR activity						*z*	*y*	*x*

[a] The Bravais primitive cell contains two molecules; N_i = internal modes within molecules, T_a = inactive acoustic modes, T = optic translatory modes, and R = rotatory modes of $NbAlCl_8$ molecules.

Table VII. Raman Vibrational Frequencies (cm^{-1}) and Assignments for the $NbAlCl_8$ Crystal at Room Temperature[a]

crystal[b] (molecule[c])			
A_g (A_1)	B_{1g} (B_2)	B_{2g} (A_2)	B_{3g} (B_1)
			565 w
497 w	497 m		
	436 m		
422 vs	426 s		422 m?
	400 w		
364 vs			364 m?
361 vs			
340 vw	345 m		
229 w			
186 m		173 s	191 m
157 s	143 w		165 s
117 m	117 m	128 m	128 m
105 w	74 w	84 m	84 w
	50 m	50 m	40 m
			27 m

[a] Key: w = weak; m = medium; v = very; s = strong; ? = perhaps band leaking from other orientation. [b] Orientation of axes in the crystal; see Table V. [c] Orientation of axes in the molecule; see Table IV.

the direction of collection of Figure 5 experiments most probably was along *a*. The following interpretation is in accordance with this assumption. The polarization of the exciting beam then could be along the *a* or *c* axes and the collection polarization along the *b* or *c* axes (the crystal orientations are indicated in Figure 5 in the standard nomenclature relating to crystal axes: [*x*(*yz*)*q*], where *x* = excitation direction, *y* = excitation polarization, *z* = collection polarization, and *q* = collection direction).

The number of bands to be found in the different Raman experiments can be predicted by the standard group-theoretical analysis.[28] One $NbAlCl_8$ molecule of C_{2v} point symmetry has 24 internal vibrational modes (in addition to the translations and rotations). The vibrations transform according to $\Gamma_{vib} = 9A_1 + 3A_2 + 6B_1 + 6B_2$ and are all Raman active. The distribution of these on internal group vibrations is shown in Table IV. Of course, some of these vibrations might couple with others of the same symmetry and make the distribution in Table IV more or less meaningless, but still Table IV might give some information on the number of bands to be seen in the bond-stretching range (ca. 600–200 cm^{-1}) and in the deformation–translation–rotation range (below ca. 200 cm^{-1}).

The primitive Bravais cell of the crystal contains two $NbAlCl_8$ molecules at sites of C_{2v} symmetry. Dynamic correlation coupling between the two molecules results in a theoretical doubling of the number of crystal fundamentals, as compared to the number in the isolated molecule. The centrosymmetry of the crystal, on the other hand, excludes half of the modes (the ungerade ones) from Raman activity. The detailed correlation diagram is shown in Table V. Finally, the external (lattice) modes should be included in the analysis.[29,30] The translations ($A_1 + B_1 + B_2$) and rotations ($A_2 + B_1 + B_2$) of the isolated C_{2v} molecule in the crystal create three acoustic, three translatory, and six rotary modes. The whole analysis is summarized in Table VI.

From this information, the spectra in Figure 5 can be assigned as shown in Table VII. The orientation of the crystal (sitting inside the ampule) was difficult to adjust properly, and the light was collected over a wide cone, so the separation of the modes among the different orientations cannot be expected to be perfect. Leaking bands are labeled with asterisks in Figure 5. Two assignment problems (Fermi resonance?) are worth being mentioned: The B_{1g} spectrum seems to contain an extra band in the 500–300-cm^{-1} range and the B_{3g} mode at 565 cm^{-1} seems very high. The B_{3g} chloride stretchings apparently are weak.

In order to be sure of the identity of the crystals and to be sure that the samples did not deteriorate under the illumination, we remeasured room-temperature spectra of nonoriented $NbCl_5$ and $AlCl_3$ crystals (Figure 6). Our spectra were in perfect accordance with the scattered information in the literature.[31-34] The bands as measured on our instrument (in

---

(28) See, e.g.: Fateley, W. G.; McDevitt, N. T.; Bentley, F. F. *Appl. Spectrosc.* **1971**, *25*, 155.

(29) Adams, D. M. *Coord. Chem. Rev.* **1973**, *10*, 183.

(30) Adams, D. M.; Newton, D. C. "Tables for Factor Group and Point Group Analysis"; Beckman-RIIC Ltd.: Croydon, England, 1970.

(31) Werder, R. D.; Frey, R. A.; Günthard, H. H. *J. Chem. Phys.* **1967**, *47*, 4159.

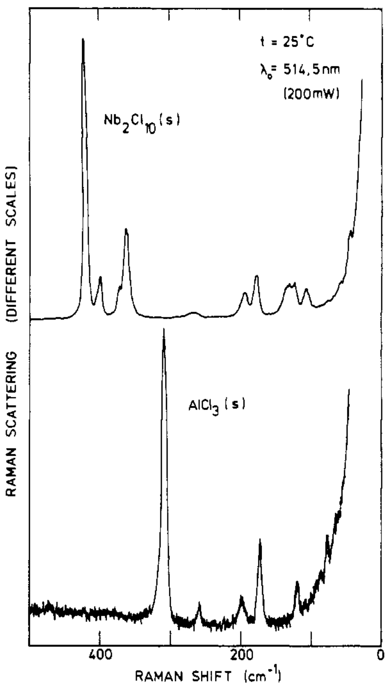

Figure 6. Raman spectra of polycrystalline Nb$_2$Cl$_{10}$ and AlCl$_3$ (resolution ~2 cm^{-1}).

cm^{-1}) occurred as 416 vs, 396 s, 370 m, 359 s, 264 w, 191 m, 174 s, 133 m, 127 m, 120 s, 104 m, and 42 m in "Nb$_2$Cl$_{10}$" and as ~308 s, 257 w, 196 w, 171 m, 118 w, and 76 w in AlCl$_3$ (see Figure 6). The complete absence of the strongest of these bands (416 and 308 cm^{-1}) from the NbAlCl$_8$ spectra (and the stability of these) is in accordance with the NbAlCl$_8$ molecular concept of interpretation.

A similar result regarding the existence of NbGaCl$_8$ has been obtained by Okon,[14] who examined the Raman spectra of the polycrystalline solid and of melts. The spectrum of the NbGaCl$_8$ solid obtained by Okon is very much like our NbAlCl$_8$ spectra. Such invariance of Raman spectra toward aluminum–gallium substitutions has been found previously,[35] and thus our crystallographic results support Okon's NbGaCl$_8$ molecular interpretation.

Complexation in Molten Mixtures of NbCl$_5$–AlCl$_3$

Melts of pure niobium pentachloride and pure aluminum chloride are known to consist of molecules (Nb$_2$Cl$_{10}$ in equilibrium with NbCl$_5$ and Al$_2$Cl$_6$, respectively), and the Raman spectra of the melts are well characterized.[32,33,36–38] Molten binary mixtures of NbCl$_5$ and AlCl$_3$ have been investigated only by Huglen et al.,[36] who recorded Raman spectra of several NbCl$_5$–AlCl$_3$ molten mixtures between 140 and 270 °C and compared the spectra with those of the pure molten components. They concluded that at ~200 °C the system should contain noninteracting molecules of NbCl$_5$, Nb$_2$Cl$_{10}$, and Al$_2$Cl$_6$.

We have repeated and extended these Raman measurements for three different mixtures as well as for the pure components. The color of the mixtures was yellow-brown, similar to that of the NbCl$_5$ melts. The cells were made from borosilicate tubing and were placed in a water-cooled, high-temperature furnace with four separately heated windows.[27] The temperature was measured with a calibrated chromel–alumel thermocouple at the cell surface. Spectra were obtained with the instrumentation described above and are shown in Figure 7. Our spectra do not deviate much from those reported by Huglen et al.[36] However, our interpretation is basically different. The strong NbAlCl$_8$ Raman bands at ca. 424 and 363 cm^{-1}, characteristic of the molecules when they are solidified,

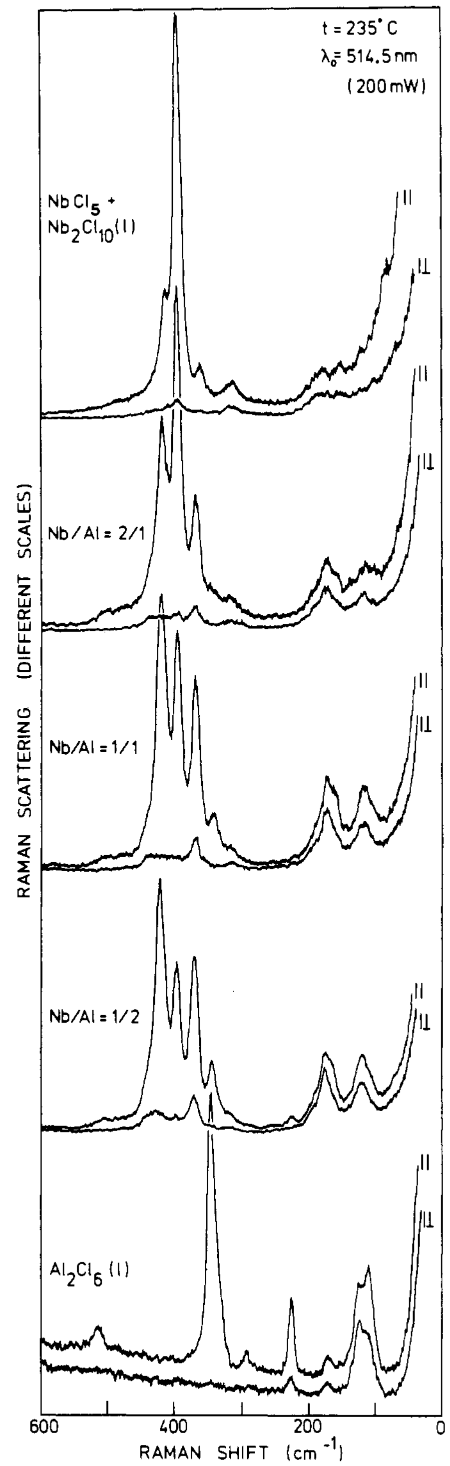

Figure 7. Raman spectra of molten niobium pentachloride, aluminum trichloride, and mixtures thereof, showing the formation of NbAlCl$_8$ (resolution ~3 cm^{-1}). Essentially similar spectra were obtained with use of red light (λ_0 = 647.1 nm, independent of power), but for green light at higher/lower power or at higher/lower temperatures, the bands at 416 and 364 cm^{-1} lost/gained intensity relative to that of the 393-cm^{-1} band.

---

(32) Beattie, I. R.; Gilson, T. R.; Ozin, G. A. *J. Chem. Soc. A* **1968**, 2765.
(33) Bues, W.; Demiray, F.; Øye, H. A. *Z. Phys. Chem.* (*Wiesbaden*) **1973**, *84*, 18.
(34) Huglen, R.; Poulsen, F. W.; Mamantov, G.; Marassi, R.; Begun, G. M. *Inorg. Nucl. Chem. Lett.* **1978**, *14*, 167.
(35) Berg, R. W.; Bjerrum, N. J. *Polyhedron* **1983**, *2*, 179.
(36) Huglen, R.; Mamantov, G.; Smith, G. P.; Begun, G. M. *J. Raman Spectrosc.* **1979**, *8*, 326.
(37) Torsi, G.; Mamantov, G.; Begun, G. M. *Inorg. Nucl. Chem. Lett.* **1970**, *6*, 553.
(38) Øye, H. A.; Rytter, E.; Klaeboe, P.; Cyvin, S. J. *Acta Chem. Scand.* **1971**, *25*, 559.

Table VIII. Raman Spectral Data (cm^{-1}) for the Molten $NbCl_5$-$AlCl_3$ System at 235 °C (Figure 7)[a]

"$NbCl_5$"	"$NbCl_5$"/ "$AlCl_3$" = 1/1	"$AlCl_3$"	molecular origin
		602 w, dp	Al_2Cl_6
		508 w, p	Al_2Cl_6
	~500 w, p		$NbAlCl_8$
	~438 w, dp		$NbAlCl_8$
	416 s, p		$NbAlCl_8$
412 w, p			Nb_2Cl_{10}
393 s, p	392 s, p		$NbCl_5$, Nb_2Cl_{10}
	364 s, dp, p		$NbAlCl_8$
358 w, p			$NbCl_5$, Nb_2Cl_{10}
	339 w, p	339 s, p	Al_2Cl_6
310 w, dp	~311 w, dp		$NbCl_5$
		~283 w, p	Al_2Cl_6
		218 m	Al_2Cl_6
	~190		$NbAlCl_8$
176 w, dp			$NbCl_5$
	~168 m, dp		$NbAlCl_8$
		165 w, dp	Al_2Cl_6
	~156 m, p		$NbAlCl_8$
151 w, dp			$NbCl_5$
	~113 m, dp		$NbAlCl_8$
		~118 m, dp	Al_2Cl_6
		103 m	Al_2Cl_6

[a] Key: p = polarized, dp = depolarized.

are clearly discernible in the molten $NbCl_5$–$AlCl_3$ mixtures (at 416 and 364 cm^{-1}). Therefore, our interpretation considers the molten mixtures to consist of $NbCl_5$, Nb_2Cl_{10}, Al_2Cl_6, *and* $NbAlCl_8$ molecules in concentrations determined by the composition and the temperature. Huglen et al.[36] explained the bands at ca. 420 and ca. 368 cm^{-1} in their mixtures as due to $NbCl_5$ + Nb_2Cl_{10}, and although these molecules have bands in the neighborhood, this interpretation would require significant composition-dependent changes in band positions and intensities *and* a change in the depolarization ratio for the ca. 364-cm^{-1} band, relative to the spectrum of the pure niobium pentachloride melt at the same temperature. Our postulated formation of molecular $NbAlCl_8$ in the melts is a much more satisfying explanation of the spectroscopic evidence (see Table VIII).

The Vapor-Phase Complex

Since a large number of halide gas complexes,[2,3] including $UAlCl_8$,[11,39] have been characterized by mass spectroscopy or other spectroscopic methods, we tried to prove the existence of the present compound as a species in the gas phase by means of Raman and mass spectroscopy. Previously, such a complex was not detected by visible spectroscopy of a gaseous mixture of $NbCl_5$ + Al_2Cl_6 at 300 °C, probably due to almost similar spectra for $NbCl_5$ and $NbAlCl_8$ and due to a small conversion of $NbCl_5$ to $NbAlCl_8$ under the examined conditions.[16]

Vapor Raman Spectra. Several gas-phase cells were prepared having varying amounts of $AlCl_3$ and $NbCl_5$. The chemicals were sublimed into the cells, and the Raman measurements were made with use of the furnace and techniques described above as well as elsewhere.[27] Measurements from two cells containing vapor mixtures will be presented here. Other cells gave similar results and do not contribute to the discussion. All cells were approximately of the same dimensions with a volume of ~5 cm^3. Cell I had 97 mg of $AlCl_3$ plus 226 mg of $NbCl_5$; cell II had 150 mg of $AlCl_3$ plus 30 mg of $NbCl_5$. Two additional cells containing pure $AlCl_3$ and pure $NbCl_5$ were also prepared.

At temperatures above 220 °C (and under the assumption that $AlCl_3$ and $NbCl_5$ do not interact), all the $AlCl_3$ contained in cells I and II should be in the vapor phase (as Al_2Cl_6), giving rise to pressures of ~3 and ~4.5 atm, respectively. At the same temperature $NbCl_5$ should be liquid with a vapor pressure of ~0.5 atm (boiling point of $NbCl_5$ ~250 °C).[19] However, heating cells I and II above 200 °C resulted in the formation of yellow-brown liquids, which were present at temperatures even above 350 °C. Presumably,[19] in these cells the partial pressures of the components (Al_2Cl_6, $NbCl_5$) are lower than the pressures calculated from the added amounts of chemicals. Thus, a study of vapor complexation by variation of the temperature and Al_2Cl_6(g) pressure by the use of Raman or absorption spectroscopy[2] cannot be easily achieved.

However, the Raman spectra obtained here over the stable liquid (mixture) give evidence of the formation of vapor complexes. Figure 8 presents the Raman spectra obtained at 300 °C from cells I and II. The spectra of gaseous niobium pentachloride[33,40] and aluminum chloride[27a,41,42] are well-known and are included in Figure 8 for the purpose of comparison. At ca. 300 °C, niobium pentachloride is predominantly monomeric, having its strongest Raman band at 394 cm^{-1},[33,40] and aluminum chloride is dimeric, having characteristic bands at e.g. 340, 331, and 218 cm^{-1}.[27a,41,42]

Spectra in parts B and C of Figure 8 are superpositions of bands due to $NbCl_5$(g) and Al_2Cl_6(g). Two new bands at 418 and 369 cm^{-1} (arrows in Figure 8) are presumably due to new vapor species. These bands were best observed at lower temperatures in cell II (having higher partial pressure of Al_2Cl_6) as shown in Figure 9B. At ~235 °C the intensity of the band at 394 cm^{-1} due to $NbCl_5$(g) is comparable in magnitude to that of the band at 418 cm^{-1} (and the shoulder at 369 cm^{-1}) due to the vapor complex(es). It is interesting to note how little the $NbAlCl_8$ strong bands shift from the crystalline phase (ca. 422 and ca. 363 cm^{-1} at 25 °C) over the liquid phase (ca. 416 and ca. 364 cm^{-1} at 235 °C) to the gas phase (ca. 418 and 369 cm^{-1} at 300 °C). This serves to prove that the identity of the complex is retained in all three phases.

The 418-cm^{-1} $NbAlCl_8$ band was followed with respect to temperature (Figure 9). Even at 235 °C, the liquid $NbCl_5$ band at ca. 414 cm^{-1} [33] was not found to be present in the gas phase (Figure 9A), showing that Nb_2Cl_{10} dimers can be excluded from the considerations. The intensity of the 418-cm^{-1} $NbAlCl_8$ band decreased with increasing temperature, relative to the 394-cm^{-1} $NbCl_5$ band and relative to the Al_2Cl_6 bands (compare Figure 8C with Figure 9E). This can be interpreted in terms of a dissociation of the gas complex according to

$$2NbAlCl_8 \rightarrow Al_2Cl_6 + 2NbCl_5$$

At 350–400 °C vanishing amounts of gas complex were left (Figure 9E). It is noteworthy that the spectra shown in parts A (pure $NbCl_5$(g)) and B (vapor mixture) of Figure 9 were obtained under the same conditions (laser power, geometry of optics, position of cells), and thus relative intensities from cell to cell can be determined with an estimated error of $\lesssim$5%. It thus appears, from the intensity of the $NbCl_5$(g) band at 394 cm^{-1}, that the partial pressure of $NbCl_5$(g) over the stable liquid mixture is approximately 10 times lower than the vapor pressure over pure $NbCl_5$(l).

Finally, measurements of the vapor Raman spectra using different laser powers showed no changes in the relative intensities of the observed bands. On the other hand, changing the laser light frequency from red to blue altered the intensities of the $NbCl_5$(g) and $NbAlCl_8$(g) bands relative to those of the Al_2Cl_6(g) bands. As the frequency was changed from λ_0 = 647.1 nm to λ_0 = 488.0 nm, the intensities of the ~418-

---

(39) Papatheodorou, G. N.; Buttry, D. A. *Inorg. Nucl. Chem. Lett.* **1979**, *15*, 51.

(40) Beattie, I. R.; Ozin, G. A. *J. Chem. Soc. A* **1969**, 1691.

(41) Beattie, I. R.; Horder, J. R. *J. Chem. Soc. A* **1969**, 2655.

(42) Maroni, V. A.; Gruen, D. M.; McBeth, R. L.; Cairns, E. J. *Spectrochim. Acta, Part A* **1970**, *26A*, 418.

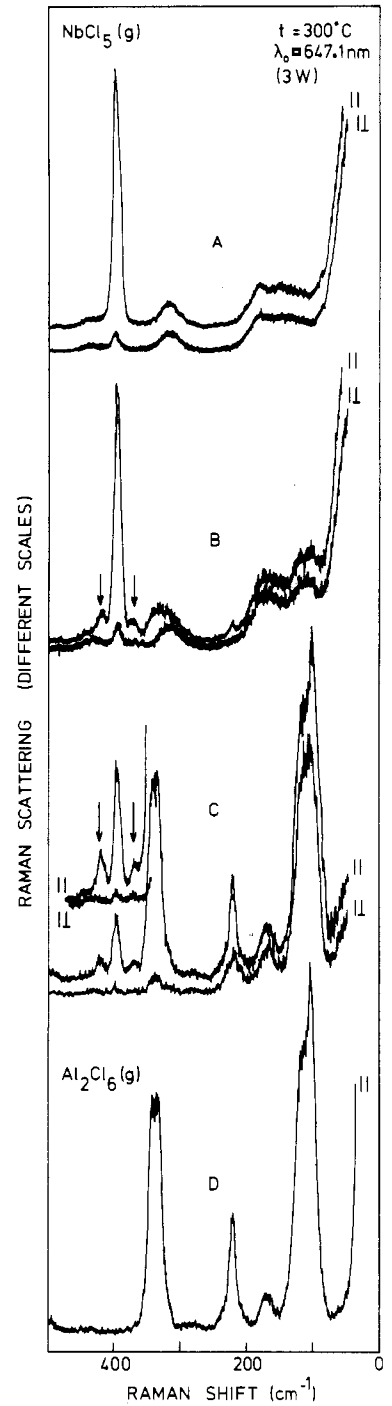

Figure 8. Gas-phase Raman spectra of vapors over melts of niobium pentachloride (A), aluminum trichloride (D), and mixtures in cell I (B) and in cell II (C), showing the formation of $NbAlCl_8$ (arrows) (resolution ~6 cm^{-1}). Essentially similar spectra were obtained with use of green or blue light at different power levels.

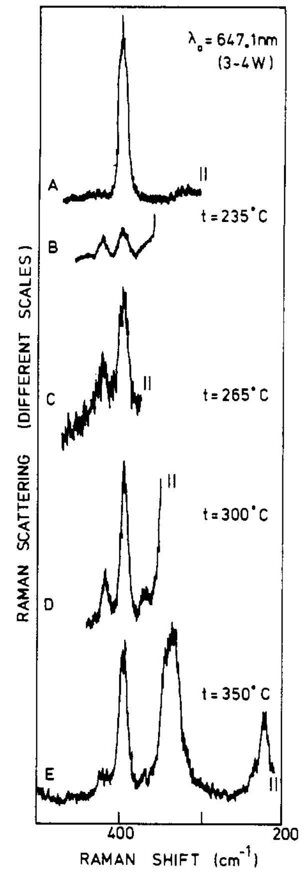

Figure 9. Temperature dependence of Raman spectrum of $NbAlCl_8$ (resolution ~6 cm^{-1}): (A) pure $NbCl_5$(g); (B–E) $NbAlCl_8$(g) in equilibrium with $NbCl_5$(g) and Al_2Cl_6(g) over liquid phase (cell II).

and ~394-cm^{-1} bands were almost tripled relative to those of Al_2Cl_6(g). This indicates preresonance enhancement of the $NbCl_5$(g) and $NbAlCl_8$(g) fundamentals due to overlap of the excitation line with the tail of the UV-absorption bands of the niobium vapor species.

Mass Spectra. The mass spectra were recorded with a VARIAN MAT CH5 instrument at sample temperatures of 40 and 65 °C and with electron energies of 20 and 70 eV. A typical spectrum of solid $NbAlCl_8$ (70 eV, 65 °C) shows peaks of Al^+ (relative intensity 16), Cl^+ (28), $AlCl^+$ (19), $NbCl_2^{2+}$ (12), Nb^+ (46), $AlCl_2^+$ (81), $NbCl_3^{2+}$ (58), $NbCl_4^{2+}$ (1), $NbCl^+$ (45), $AlCl_3^+$ (46), $NbCl_2^+$ (53), $NbCl_3^+$ (50), $Al_2Cl_5^+$ (37), and $NbCl_4^+$ (100). Only minute quantities (less than 10^{-4} relative to the most intense fragment $NbCl_4^+$) of the relevant fragments $NbAlCl_6^{2+}$ and $NbAlCl_7^+$ were observed.

Our mass spectra support the previous results of double-cell mass spectrometric investigations[12] on $NbCl_5$–Al_2Cl_6 mixtures; the existence of $NbAlCl_8$ (and the homologous $TaAlCl_8$) was argued from extremely small fragment intensities. The lability may be related to the relative weak Nb–Cl bridge bonds as evidenced by the structural results of the solid.

The failure of mass spectrometry to definitively identify weakly bound vapor complexes is not surprising because of the extremely low pressure conditions under which these experiments are conducted. In contrast to this, the vapor Raman measurements, obtained on closed cells under equilibrium conditions and at much higher pressures of the reacting gases, appear to be much more successful in pointing out the formation of complexes. Furthermore, Raman spectroscopy can be useful for suggesting a structure for the vapor complex molecules if the crystal structure and vibrational spectra of the compound in the solid state are known (as is the case here).

Acknowledgment. B.K. and G.N.P. thank the Danish Natural Science Research Foundation for grants during stays at the Technical University of Denmark in support of the research reported here. Financial assistance by the Fonds der Chemischen Industrie and the Carlsberg Foundation is gratefully acknowledged.

Registry No. $NbAlCl_8$, 87969-73-1; $NbCl_5$, 10026-12-7; $AlCl_3$, 7446-70-0; Nb_2Cl_{10}, 17499-28-4; Al_2Cl_6, 13845-12-0.

Supplementary Material Available: Tables of intermolecular Cl···Cl distances and of observed and calculated structure factors (5 pages). Ordering information is given on any current masthead page.